International Journal of Environmental Sciences
ISSN: 2229-7359
Vol. 11 No. 24s,2025
https://theaspd.com/index.php

Synthesis, Spectra And Biological Evaluation Studies Of Fe(II), Cd(II), Mn(II), Co(II), Ni(II), Zn(II), Pd(II), Hg(II) And Cu(II) Complexes With 6-Chloro-2-Aminobenzothiazole Derivatives

Dipti D. Gharat[1], Kirti P. Mhatre[2], Shailesh A. Tawde[3], Ramesh S. Yamgar[3], Shashikant D. Ajagekar[2*]
[1]Department of Chemistry, Thakur College of Science and Commerce, Kandivali East, Mumbai, Maharashtra, India-400 101
[2]Department of Chemistry, VWTCT'S Bhaskar Waman Thakur College of Science, Virar West, Maharashtra, India-401303
[3]Department of Chemistry, CS's S.S. & L.S. Patkar College of Arts & Science, and V. P. Varde College of Commerce & Economics, Goregaon, Mumbai, India-400062.
*Corresponding Author: drsdajagekartcsc@gmail.com

Abstract
Metal complexes of the type [M(AMBTDH)$_2$], (M = Fe(II), Cd(II), Mn(II), Co(II), Ni(II), Zn(II), Pd(II), Hg(II) and Cu(II)) of HAMBTDH (4-{[(6-chloro-1,3-benzothiazol-2-yl)imino]methyl}benzene-1,3-diol) ligand, have been synthesized and characterized by elemental analysis, NMR, infrared, electronic absorption, mass, magnetic moments, Xrd, and ESR spectroscopic methods. Based on the spectrum data, a square planar geometry is proposed for the Pd(II) complex; tetrahedral geometry is proposed for the Hg(II), Cd(II), and Zn(II) complexes; and high spin octahedral in nature is proposed for the other complexes. The low molar conductance values in nitrobenzene indicate that the metal complexes are non-electrolytes. Additionally, the antimicrobial activities of the all-prepared compounds were investigated and analysed as part of this investigation.
Keywords: *Metal complexes, biological activity, Square planar, Tetrahedral and Octahedral geometry.*

1. INTRODUCTION:

The structures and potential applications of transition metal complexes containing Schiff base ligands [1-4] have been intensely studied for many years. Benzothiazole is one example. These days, scientists can't get enough of studying Schiff base complexes [5, 6]. Researchers have paid much attention to the coordination chemistry of bi-dentate Schiff bases with N and O donor ligands. Because of their unique ligation behaviour and chelating capacity, azomethine derivatives are greatly interested in coordination chemistry. Extra donor sites, such as a -OH group, can be found in the ligands. They're more adaptable and flexible attributable to the extra donor locations. These ligands possess a wide variety of biological characteristics, including antifungal [7-9], antibacterial [10], and anticancer [11, 12] actions, and can react with metals in either their neutral or monoanionic states. Electrostatic, groove, intercalative, and partial intercalative binding modes, including non-covalent interactions with DNA, are synthesised with the help of transition metals. Intercalation has become prominent due to its potential uses in cancer treatment and molecular biology [14–17].

DNA's properties as a biological receptor make its binding nature with transition metal complexes an active area of study. Biological effects, such as the anticancer impact through DNA binding, are often observed with transition metal complexes. Changes in DNA replication and the suppression of tumour cell proliferation are just two of the many results of this phenomenon. Because of this, more and better anticancer medicines have been available, the efficacy of which is highly dependent on affinity and mechanism of binding. In addition to their physicochemical features, Co(II), Ni(II), and Cu(II) complexes also display a wide variety of biological activities [18–20]. In consideration of the preceding, we provide herein the results of investigations on the synthesis and characterisation of 2, 3-dihydroxybenzaldehyde derivatives of 6-methoxy-2-aminobenzothiazole (HAMBTDH) ligand and its transition metal complexes, as well as their antifungal and antibacterial properties.

MATERIALS AND METHODS:

Sigma-Aldrich, Merck, and BLD Pharma supplied all the solvents and reagents. The Schiff bases and their metal complexes were analysed using a Perkin Elmer 240C elemental analyzer to determine their individual carbon, hydrogen, nitrogen, and sulfur content percentages. The Bruker IMPACT HD mass

spectrometer was used to perform mass spectrometry. The Schiff base NMR spectra were acquired with a Bruker 400 MHz NMR apparatus with a TMS standard. Electronic absorption spectra were taken in DMF using a JASCO V650 UV-visible spectrophotometer. Brucker FT-IR spectrometer on KBr pellets was used to record FT-IR spectra in the range 4000-500 cm^{-1}. Using $Hg[Co(NCS)_4]$ as a standard, the magnetic moments of the complexes were measured on a Gouy balance, and their diamagnetic corrections were established using Pascal's constants. The JES - FA200 ESR Spectrometer with a Q band acquired the spectra at room temperature. Powder X-ray diffraction analysis was performed by BRUKER D8 VENTURE instrument with Cu–Kα radiation (wavelength 0.154 nm) operating at 40 kV and 30 mA. Measurements were scanned for diffraction angles (2θ) ranging from 20 o to 90◦ with a step size of 0.02◦ and a time per step of 1 s.

Synthesis of HAMBTDH ligand:

The method for synthesizing the ligand is outlined in **Scheme 1**. A round bottom flask containing a 10 mM ethanolic solution of 6-methoxy-2-aminobenzothiazole was subjected to magnetic stirring. Subsequently, a 10 mM ethanolic solution of 2, 3-dihydroxybenzaldehyde was added dropwise to the flask in a 1:1 ratio. The reaction mixture underwent reflux at 50-60 °C temperature while continuously stirring for 3.5 hours. The advancement of the reaction was observed using thin-layer chromatography (TLC). The solution was allowed to cool to ambient temperature. Afterwards, the solid product with a yellow solid was separated and subjected to a purification process involving cold ethanol and petroleum ether washes. The Schiff bases were subjected to vacuum drying using desiccators containing anhydrous $CaCl_2$.

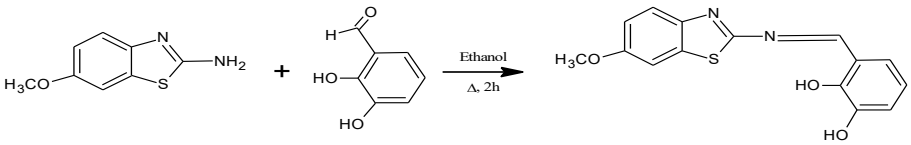

Scheme-1: Preparation of HAMBTDH

Synthesis of metal (II) complexes:

As the hot ethanolic solution of HAMBTDH ligand (10 mM) was being agitated, a drop-by-drop addition of a hot ethanolic solution of metal sulphates (5 mM) was prepared. The colour developed in the solution as it was being added. A dilute alkali was used to get the pH level up to 7. We next filtered and washed the acquired solid product with hot ethanol to remove any impurities. Vacuum desiccators dehydrated the metal complexes in an anhydrous $CaCl_2$ solution.

Antimicrobial activity:

The HAMBTDH ligand and its complexes were tested for antimicrobial activity using the disc diffusion method on a nutrient agar plate [21-22]. Two Gram-positive bacteria, *B. subtilis, S. aureus* and two Gram-negative bacteria, *Escherichia coli* and *P. aeruginosa*, were used to test the antibacterial activity in vitro. Similarly, two fungi, *S. cerevisiae* and *C. albicans*, were used to test the antifungal activity. The standards for antibacterial and antifungal drugs were *streptomycin* and *fluconazole*, respectively. For each compound, a stock solution with a 500 g/mL concentration was made by dissolving 5 mg of the sample in 10 mL of DMSO. After setting the dishes aside for an hour, the drug solution diffused more easily throughout the dish. The zone of inhibition was then measured in millimetres after the plates were incubated at 37°C for 24 hours for bacteria and 48 hours for fungi. After incubation for 24 hours at 37°C, the concentration (mg/mL) of chemical that inhibits bacterial growth was determined. None of the microorganisms examined were affected by increasing the DMSO content in the medium.

***In vitro* cytotoxicity:**

Synthesized HAMBTDH ligand and complexes of Mn(II), Fe(II), Co(II), Ni(II), Pd(II), Cu(II), Zn(II), Cd(II), and Hg(II) were investigated for cytotoxicity (brine shrimp bioassay) [23]. Eggs for shrimp were placed in one half of a tank that had been divided in half and then filled with artificial seawater (38 g NaCl/1000 mL tap water). The eggs were allowed to hatch into nauplii within 48 hours. The newborn shrimp were collected to be used in a bioassay. The test tubes included varying amounts of dried complexes (2.5, 7.5, 10, and 12.5 mg/10 mL). The cytotoxic potential of the complexes was evaluated by dissolving DMSO in them. A Pasteur pipette transferred 10 living shrimp to each test tube. A control group was included to ensure the testing protocol and results for the agent's cytotoxic activity were accurate. After 24 hours, the tubes were examined under a microscope to count the surviving nauplii and record other relevant observations. There were three sets of five replicates for each experiment. We determined the LC50, 95% confidence limit, LC90, and chi-square using the collected data. Abbott's

method [24] was used to adjust the data to account for the occurrence of control fatalities. % deaths = [(test-control)/control] x 100.

RESULTS AND DISCUSSION:

There is colour and room-temperature stability in the HAMBTDH ligand and its metal complexes. Methanol, acetonitrile, chloroform, DMSO, DMF, DCM, etc., are all organic solvents compatible with HAMBTDH ligands. It has been determined that all of the complexes are insoluble in water but soluble in DMF, nitrobenzene and DMSO. All synthesized complexes provide analytical data that agrees well with projected values for 1:2 metal-to-ligand stoichiometric ratios. At room temperature, the molar conductance of the complexes in nitrobenzene (10^{-3} M solutions) was measured, and the results are shown in **Table 1,** indicating they are non-electrolyte in nature [25].

Table-1: Physico-chemical and analytical data of HAMBTDH ligand and its metal complexes

Comp	Colour	MW	% Yield	MP/DP	Element Content						Cond	MM
					M	C	H	N	O	S		
HAMBTDH	Yellow	300.33	74.69	180	-	59.99	4.03	9.33	15.98	10.68	-	-
Fe(AMBTDH)$_2$	Blue	654.55	88.69	205	8.54	55.05	3.36	8.56	14.68	9.79	2.25	5.16
Co(AMBTDH)$_2$	Brown	659.65	74.62	200	8.94	54.57	3.34	8.49	14.60	9.70	3.91	4.39
Ni(AMBTDH)$_2$	Orange	659.35	78.76	201	8.90	54.60	3.34	8.49	14.60	9.71	9.91	2.96
Pd(AMBTDH)$_2$	Orange	706.66	80.91	205	15.00	50.94	3.11	7.93	14.60	9.06	0.85	-
Cu(AMBTDH)$_2$	Green	664.21	82.26	206	9.57	54.20	3.31	8.43	14.50	9.64	1.71	2.13
Zn(AMBTDH)$_2$	Yellow	666.05	76.97	205	9.82	54.05	3.30	8.41	14.40	9.61	2.87	-
Cd(AMBTDH)$_2$	Yellow	713.07	68.30	209	15.77	50.49	3.09	7.85	13.50	8.98	0.83	-
Hg(AMBTDH)$_2$	Red	800.66	74.14	212	25.05	44.96	2.75	6.99	11.99	7.99	1.88	-
Mn(AMBTDH)$_2$	Brown	653.59	76.13	200	8.41	55.08	3.37	8.58	14.70	9.79	1.74	5.31

FT(IR) spectroscopy:

Table 2 summarises the significant infrared (IR) bands observed in the ligand and its metal (II) complexes, along with their recommended assignments. The infrared spectra of the unbound HAMBTDH ligand exhibited a distinct peak at 3068 cm^{-1}, which can be attributed to the presence of a phenolic –OH group. This peak was absent in the spectra of the corresponding metal complexes, suggesting that the phenolic –OH group undergoes deprotonation upon the formation of the complexes. Complexes exhibited a pronounced and wide peak within the 3224-3422 cm^{-1} spectral region. This peak can be attributed to a second hydroxyl (OH) group in the meta position relative to the phenolic –OH group [26]. The confirmation of the coordination of the phenolic –OH group is supported by the observed shift of a band from 1160 cm^{-1} (HAMBTDH) to a lower frequency range of 1121-1156 cm^{-1}. This shift is attributed to the stretching frequency of the C–O group of the HAMBTDH ligand [27, 28]. The stretching frequency of the azomethine (–C=N) in the Schiff base experiences a downward shift of 7–18 cm^{-1} during complexation, indicating the coordination of the azomethine nitrogen to the metal ion [29, 30]. Furthermore, two additional bands were observed in the lower frequency area between 535-607, 511-537 cm^{-1} and 507-514 cm^{-1}. These bands can be attributed to the stretching frequency of the M→N, M→S and M-O bonds [21-24]. The appearance of these bands provides further evidence supporting the coordination of the complexes, as depicted in **Figure 1**.

Table 2: FT(IR) spectral data of HAMBTDH ligand and its metal complexes

Comp	-OH (C4)	-OH (C2)	-OCH_3	-CH=	>C=N-	C-O	Ar-OH	C-S	N→M	S→M	O-M
HAMBTDH	2999	3068	2944	2905	1637	1330	1160	1218	-	-	-
Fe(AMBTDH)$_2$	3397	-	2943	3068	1582	1328	1156	1217	579	534	507
Co(AMBTDH)$_2$	3416	-	2997	3068	1582	1318	1121	1217	559	559	514
Ni(AMBTDH)$_2$	3422	-	3000	3069	1537	1348	1126	1217	580	560	532
Pd(AMBTDH)$_2$	3397	-	3068	2942	1636	1328	1124	1217	579	579	502
Cu(AMBTDH)$_2$	3326	-	2922	2830	1636	1277	1123	1225	588	588	515
Zn(AMBTDH)$_2$	3270	-	3033	2919	1631	1303	1126	1208	607	-	511
Cd(AMBTDH)$_2$	3391	-	2921	2850	1580	1308	1152	1214	535	-	516
Hg(AMBTDH)$_2$	3381	-	3187	2796	1655	1326	1123	1226	544	-	518
Mn(AMBTDH)$_2$	3224	-	3150	3033	1632	1302	1124	1204	606	537	511

ESR spectra:

The electron spin resonance (ESR) spectra of the [Cu(AMBTDH)$_2$] complex offer valuable insights into the degree of electron delocalization and the characteristics of the metal-ligand interaction. The spectra analysis reveals that the values for $g_{\parallel}$, $g_{\perp}$, and G are determined to be 2.12, 2.08, and 1.51, respectively. The observed $g_{\parallel}$ value is higher than the corresponding $g_{\perp}$ value, indicating that the [Cu(AMBTDH)$_2$] complex exhibits a distorted octahedral geometry. Furthermore, an unpaired electron localized in the d_{x2-y2} molecular orbital suggests that the complex has a $^2B_{1g}$ ground state. The number denoted as "G" in the study indicates the presence of significant trade contacts across copper centres [34]. The g-value, as indicated by the data from sources [35, 36], is less than 2.3, implying a covalent link between the metal and ligand.

UV-visible spectra and Magnetic moments:

Table 3 summarises the UV-visible spectroscopic analysis performed at room temperature on DMF solutions of the HAMBTDH ligand and its metal (II) complexes. Two distinct absorption bands, at 270-321 and 348-379 nm, were observed for the HAMBTDH. These bands correspond to the π→π* transition of the aromatic ring and the n→π* transition of the azomethine group. These bands' locations alter to shorter/longer wavelengths in metal complexes, evidence of HAMBTDH ligand coordination with metal ions. In addition, the *d - d* transition provides all complexes with a second, identifying broadband in the visible spectrum.

Since there are five unpaired electrons in the octahedral structure, the effective magnetic moment of the Fe(II) complex is 5.16 BM [37]. Absorption bands at 595nm, by the $^5T_{2g}\rightarrow{}^5E_g$ electronic transition [38], were observed in the electronic spectra of the Fe(II) complex, confirming the presence of an octahedral Fe(II) complex.

The electronic spectrum of the cobalt(II) complex includes the *d-d* transition bands at 900 and 628 nm. The $^4T_{1g}(F) \rightarrow {}^4T_{2g}(F)$ ν_1 and $^4T_{1g}(F) \rightarrow {}^4A_{2g}(F)$ ν_2, are the corresponding transitions. The octahedral geometry of the complexes is reflected in the shape of the transitions. The nickel(II) complex's absorption spectra show two *d-d* transition bands at 978 and 507 nm. These bands are denoted as follows: $^3A_{2g}(F) \rightarrow {}^3T_{2g}(F)$ ν_1 and $^3A_{2g}(F) \rightarrow {}^3T_{1g}(P)$ ν_3. These changes show that the nickel complex possesses D_{4h} symmetry and an octahedral structure [39].

The ligand field parameters Racah inter-electronic repulsion parameter B, ligand field splitting stabilisation energy 10 Dq, covalency factor, and ligand field stabilisation energy (LFSE) have all been determined for the Co(II) and Ni(II) complexes. From the transition energy ratio diagram, the values of B and Dq of Co(II) complexes were determined using the υ_3/υ_1 ratio. The evaluated values in **Table 3** consider the covalent character of the complexes being studied [40].
At 638nm, this absorption was observed in the Cu(II) complex [41]. This transition, $^2B_{1g}\rightarrow{}^2E_g$, indicates a distorted octahedral geometry enclosing copper(II). Electronic spectrum and magnetic moment measurements suggest that the Mn(II) complex has an octahedral structure. Spectra showing bands at 512 and 381 nm are compatible with octahedral geometry and correspond to the $^6A_{1g}\rightarrow{}^3T_{1g}(P)$ and $^6A_{1g}\rightarrow{}^3T_{1g}$ (F) electronic transitions, respectively [42]. The octahedral geometry of the complex is confirmed by its effective magnetic moment of 5.31 BM [43].

Table 3: Electronic spectral data of HAMBTDH ligand and its metal complexes

Compound	λnm	Transition
HAMBTDH	325	$\pi\rightarrow\pi^*$
	270	$\pi\rightarrow\pi^*$
Mn(AMBTDH)$_2$	512	$^6A_{1g} \rightarrow {}^4T_{1g}(^4P)$
	381	$^6A_{1g} \rightarrow {}^4E_g(^4D)$
Fe(AMBTDH)$_2$	595	$^5T_{2g}\rightarrow{}^5E_g$
	352, 348, 270	L → M charge transfer
Co(AMBTDH)$_2$	900	$^4T_{1g(F)} \rightarrow {}^4T_{2g(F)}$ (ν_1)
	628	$^4T_{1g(F)} \rightarrow {}^4T_{2g(P)}$ (ν_2)
Ni(AMBTDH)$_2$	978	$^3A_{2g(F)}\rightarrow {}^3T_{2g(F)}$ (ν_1)
	507	$^3A_{2g}(F) \rightarrow {}^3T_{1g}(P)$ ν_3
Pd(AMBTDH)$_2$	350, 339	L → M charge transfer
Cu(AMBTDH)$_2$	638	$^2B_{1g} \rightarrow {}^2A_{1g}$ (ν_1)
Zn(AMBTDH)$_2$	363, 348, 341	L → M charge transfer
Cd(AMBTDH)$_2$	379, 321	L → M charge transfer
Hg(AMBTDH)$_2$	371, 340	L → M charge transfer

NMR spectra:

For ^{1}H NMR spectroscopy, metal complexes were dissolved in DMSO-d_6. The HAMBTDH ligand's broad signal seen at δ12.073ppm, assigned as phenolic -OH proton (C2), this proton is missing in the Pd(II), Zn(II), Cd(II), and Hg(II) complexes. If this signal is absent, oxygen coordination has taken place, and the proton is lost during complexation. No change is seen in the spectral lines of the aromatic proton multiplets at 6.45-7.85 ppm, the aromatic -OH (C4) group singlet at 10.74-10.75 ppm, or the -CH= protons of the ring singlet at 9.23-9.24 ppm, indicating that these groups are not involved in coordination (δ).

Table 4: ^{1}H NMR spectral data of HAMBTDH ligand and its metal complexes

Comp	-OH (C2)	-OH (C4)	-CH=	-OCH$_3$	Aromatic Protons
HAMBTDH	12.07	10.74	9.23	3.89	6.44-7.85
Pd(AMBTDH)$_2$	-	10.74	9.23	3.90	6.45-7.58
Zn(AMBTDH)$_2$	-	10.73	9.24	3.90	6.44-7.59
Cd(AMBTDH)$_2$	-	10.74	9.23	3.91	6.46-7.82
Hg(AMBTDH)$_2$	-	10.73	9.24	3.88	6.45-7.81

X-Ray Diffraction:

Homo-binuclear metal complexes' X-ray diffraction was measured from 10-80 angstroms at a wavelength of 1.498. Each peak's 2 value, relative intensity, and interplanar spacing (d-values) are displayed in the accompanying data of the diffractogram. The metal complexes' average crystallite size (XRD) was determined using Scherer's formula. The crystalline phase of metal complexes was identified by the strong

peaks in the XRD patterns [44]. The average crystallite size of the copper(II), cobalt(II), nickel(II), and manganese(II) Schiff base metal complexes is 1, 21, 45, and 41 nm, respectively. Cr(III), Fe(II), Co(II), Ni(II), and Cu(II) were the $h^2 + k^2 + l^2$ values. The computed lattice parameters for metal complexes are a=7.4, b=6.59, and c=3.18. Octahedral systems could account for the reported metal complex values [45-47].

Biological activity:

Antibacterial and antifungal activity was tested for the synthesised HAMBTDH ligand and its metal complexes against two Gram-positive bacteria (*B. subtilis* (MCC 2010) and *Staphylococcus aureus* (MCC 2408)), two Gram-negative bacteria (*Pseudomonas aeruginosa* (MCC 2080) and *E. Coli* (MCC 2412)), and two fungi (*C. albicans* (MCC 1439) and *S. cerevisiae* (MCC 1033)).

Table 5 summarises the microbiological data and compares them to the gold standard in pharmaceuticals. According to **Figure 1**, the metal complexes have higher antibacterial activity than the free HAMBTDH ligand but lower activity than the standards. The atomic radius of the Cu(II) ion may explain why copper complexes have demonstrated greater biological activity than those of any other metal [48]. Metal complexes have high lipophilicity, which can be used to explain the complexes' enhanced antibacterial action [49]. According to Overtone's theory of cell permeability, the lipid membrane surrounding an organism cell selectively allows passage of only lipid-soluble molecules, making the lipophilic characteristic the master regulator of antimicrobial activity. Due to the overlapping of the ligand orbital and the partial sharing of the metal ion with donor groups, chelation also decreases the polarity of the metal ion to a greater extent. The complexes' lipophilicity improves due to increased electron delocalisation across the chelate ring. While chelation is the most important element in determining antimicrobial activity, other properties of the complexes, such as dipole moment, solubility, geometry of complexes, stereochemistry, coordination sites, concentration, and hydrophobicity, also play a role.

Table 5: Antibacterial studies of HAMBTDH ligand and its metal complexes

Compound	**Antibacterial Activity (zone of inhibition)**			
	S. aureus	***B. subtilis***	***E. coli***	***P. aeruginosa***
HAMBTDH	9	7	8	7
$Fe(AMBTDH)_2$	11	14	15	0
$Co(AMBTDH)_2$	16	15	17	12
$Ni(AMBTDH)_2$	19	16	18	15
$Pd(AMBTDH)_2$	21	15	15	12
$Cu(AMBTDH)_2$	26	24	20	19
$Zn(AMBTDH)_2$	13	18	0	6
$Cd(AMBTDH)_2$	12	13	0	19
$Hg(AMBTDH)_2$	12	13	16	17
$Mn(AMBTDH)_2$	15	16	12	9
Streptomycin	10	7	13	8

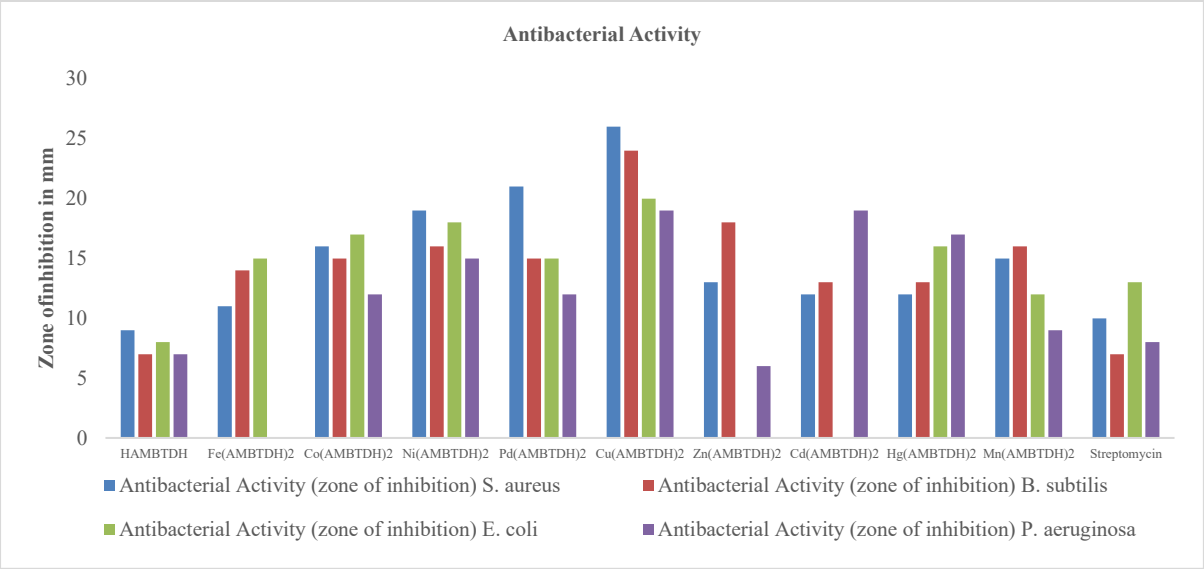

Figure 1: Antibacterial activities of HAMBTDH ligand and its complexes

Table 6: Antifungal studies of HAMBTDH ligand and its metal complexes

Compound	Antifungal Activity (zone of inhibition)	
	C Albican	***S. C.***
HAMBTDH	7	6
$Fe(AMBTDH)_2$	15	13
$Co(AMBTDH)_2$	16	17
$Ni(AMBTDH)_2$	19	20
$Pd(AMBTDH)_2$	9	11
$Cu(AMBTDH)_2$	11	9
$Zn(AMBTDH)_2$	12	10
$Cd(AMBTDH)_2$	17	11
$Hg(AMBTDH)_2$	22	9
$Mn(AMBTDH)_2$	13	18
Fluconazole	10	8

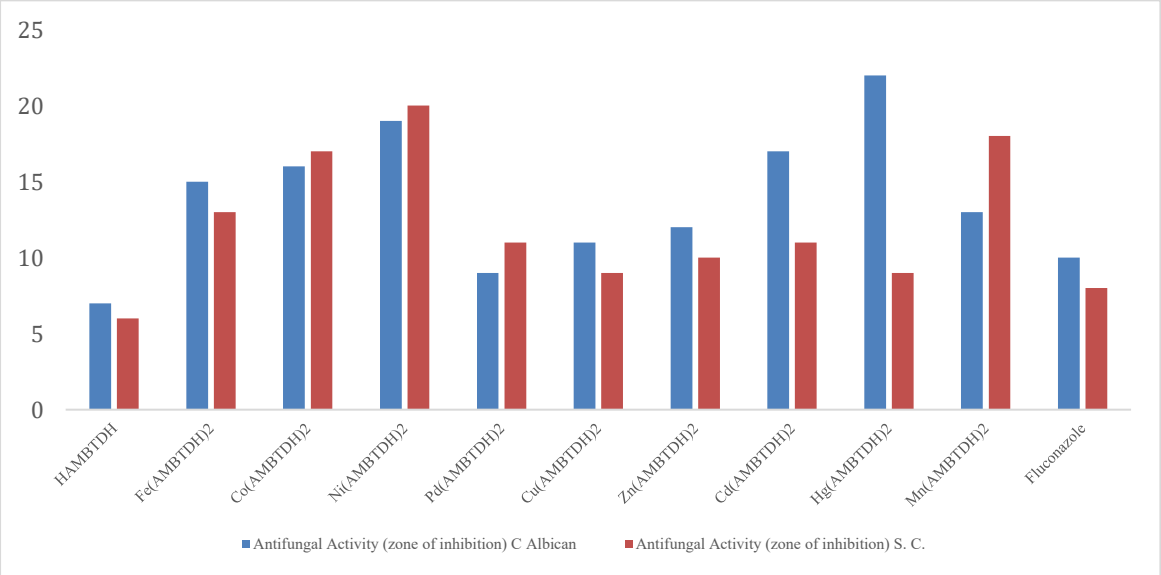

Figure 2: Antifungal activities of HAMBTDH ligand and its complexes

CONCLUSION:

Mononuclear binary metal(II) complexes of 4-{[(6-chloro-1,3-benzothiazol-2-yl)imino]methyl}benzene-1,3-diol were synthesized and characterized using a variety of spectral and analytical techniques. Based on the results, a square planar geometry is proposed for the Pd(II) complex; tetrahedral geometry is proposed for the Hg(II), Cd(II), and Zn(II) complexes; and high spin octahedral in nature is proposed for the other complexes were proposed, with coordination occurring through the azomethine's nitrogen atom and the hydroxyl group's oxygen atom. The stoichiometry of the complexes was determined to be 1:2 (metal: ligand). In conclusion, the results of the antibacterial activity investigation showed that the metal complexes are more effective than the free ligand against all the tested microorganisms. When compared to Co(II) and Ni(II) complexes, the Cu(II) complex showed the greatest antibacterial activity. Based on spectral studies, the structures of complexes are assigned as follows;

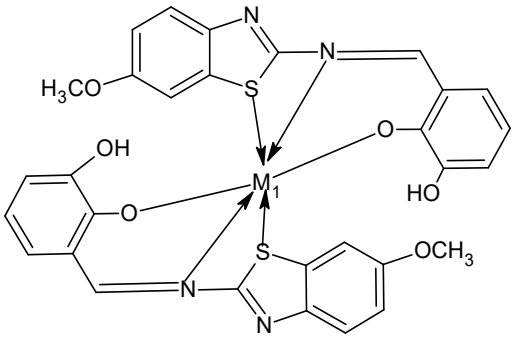

Where M_1 = Mn(II), Fe(II), Co(II), Ni(II) and Cu(II)

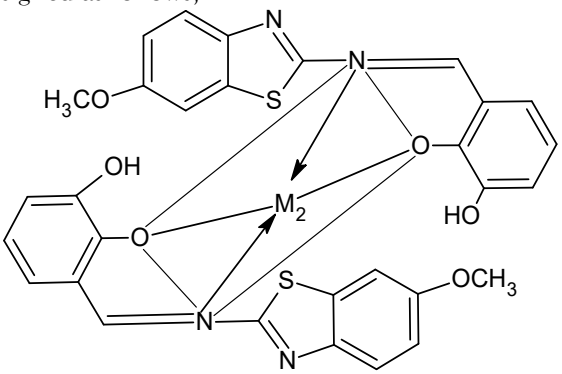

Where M_2 = Pd(II), Zn(II), Cd(II) and Hg(II)

REFERENCES:

1. Layek, S., Agrahari, B., & Pathak, D. D. (2017). Synthesis and characterization of a new Pd (II)-Schiff base complex [Pd(APD)$_2$]: An efficient and recyclable catalyst for Heck-Mizoroki and Suzuki-Miyaura reactions. *Journal of Organometallic Chemistry*, *846*, 105-112.
2. Vinayagam, V., Prabu, S., Rajalakshmi, S., & Arumugam, M. N. (2023). Synthesis, characterization, DNA interaction, antimicrobial activity, DFT analysis and molecular docking studies of copper (II) complex with triazine and neocuproine. *Journal of Molecular Structure*, *1287*, 135649.
3. Solaiman Hamed, A., & Mohammad Ali, E. (2020). Cu (II)–metformin immobilized on graphene oxide: an efficient and recyclable catalyst for the Beckmann rearrangement. *Research on Chemical Intermediates*, *46*, 701-714.
4. Matsheku, A. C., Maumela, M. C., & Makhubela, B. C. (2021). Synthesis of new adamantyl-imine palladium (II) complexes and their application in Mizoroki-Heck and Suzuki-Miyaura CC cross-coupling reactions. *Polyhedron*, *205*, 115280.
5. Al-Hamdani, U. J., Abbo, H. S., Al-Jaber, A. A., & Titinchi, S. J. (2020). New azo-benzothiazole based liquid crystals: synthesis and study of the effect of lateral substituents on their liquid crystalline behaviour. *Liquid Crystals*, *47*(14-15), 2257-2267.
6. Bikobo, D. S. N., Vodnar, D. C., Stana, A., Tiperciuc, B., Nastasă, C., Douchet, M., & Oniga, O. (2017). Synthesis of 2-phenylamino-thiazole derivatives as antimicrobial agents. *Journal of Saudi Chemical Society*, *21*(7), 861-868.
7. Ramadan, A. M., Bayoumi, H. A., & Elsamra, R. M. (2021). Synthesis, characterization, biological evaluation, and molecular docking approach of nickel (II) complexes containing O, N-donor chelation pattern of sulfonamide-based Schiff bases. *Applied Organometallic Chemistry*, *35*(12), e6412.
8. El-Tabl, A. S., El-Saied, F. A., Plass, W., & Al-Hakimi, A. N. (2008). Synthesis, spectroscopic characterization and biological activity of the Schiff base metal complexes derived from phenylaminoacetohydrazide and dibenzoylmethane. *Spectrochimica Acta Part A: Molecular and Biomolecular Spectroscopy*, *71*(1), 90-99.
9. Shukla, S. N., Gaur, P., Raidas, M. L., Chaurasia, B., & Bagri, S. S. (2021). Novel NNO pincer type Schiff base ligand and its complexes of Fe (III), Co (II) and Ni (II): Synthesis, spectroscopic characterization, DFT, antibacterial and anticorrosion study. *Journal of Molecular Structure*, *1240*, 130582.
10. Basha, M. T., Alghanmi, R. M., Shehata, M. R., & Abdel-Rahman, L. H. (2019). Synthesis, structural characterization, DFT calculations, biological investigation, molecular docking and DNA binding of Co (II), Ni (II) and Cu (II) nanosized Schiff base complexes bearing pyrimidine moiety. *Journal of Molecular Structure*, *1183*, 298-312.
11. Liu, Q., Loo, W. T., Sze, S. C. W., & Tong, Y. (2009). Curcumin inhibits cell proliferation of MDA-MB-231 and BT-483 breast cancer cells mediated by down-regulation of NFκB, cyclinD and MMP-1 transcription. *Phytomedicine*, *16*(10), 916-922.
12. Saghatforoush, L. A., Hosseinpour, S., Bezpalko, M. W., & Kassel, W. S. (2019). X-ray crystal structural and spectral studies of copper (II) and nickel (II) complexes of functionalised bis (thiosemicarbazone) ligands and investigation of their electrochemical behaviour. *Inorganica Chimica Acta*, *484*, 527-534.
13. Cardin, C. J., Kelly, J. M., & Quinn, S. J. (2017). Photochemically active DNA-intercalating ruthenium and related complexes–insights by combining crystallography and transient spectroscopy. *Chemical science*, *8*(7), 4705-4723.
14. Neto, B. A., & Lapis, A. A. (2009). Recent developments in the chemistry of deoxyribonucleic acid (DNA) intercalators: principles, design, synthesis, applications and trends. *Molecules*, *14*(5), 1725-1746.

15. Bhattacharjee, A., Das, S., Das, B., & Roy, P. (2021). Intercalative DNA binding, protein binding, antibacterial activities and cytotoxicity studies of a mononuclear copper (II) complex. *Inorganica Chimica Acta*, *514*, 119961.
16. Lippert, B., & Sanz Miguel, P. J. (2016). The Renaissance of metal–pyrimidine nucleobase coordination chemistry. *Accounts of Chemical Research*, *49*(8), 1537-1545.
17. Kellett, A., Molphy, Z., Slator, C., McKee, V., & Farrell, N. P. (2019). Molecular methods for assessment of non-covalent metallodrug–DNA interactions. *Chemical Society Reviews*, *48*(4), 971-988.
18. Yang, P., Zhang, D. D., Wang, Z. Z., Liu, H. Z., Shi, Q. S., & Xie, X. B. (2019). Copper (ii) complexes with NNO ligands: synthesis, crystal structures, DNA cleavage, and anticancer activities. *Dalton Transactions*, *48*(48), 17925-17935.
19. Singh, A., Maji, A., Mohanty, A., & Ghosh, K. (2020). Copper-based catalysts derived from salen-type ligands: synthesis of 5-substituted-1 H-tetrazoles via [3+ 2] cycloaddition and propargylamines via A 3-coupling reactions. *New Journal of Chemistry*, *44*(42), 18399-18418.
20. Mathews, N. A., & Kurup, M. P. (2021). In vitro, biomolecular interaction studies and cytotoxic activities of copper (II) and zinc (II) complexes bearing ONS donor thiosemicarbazones. *Applied Organometallic Chemistry*, *35*(1), e6056.
21. Anacona, J. R., Ruiz, K., Loroño, M., & Celis, F. (2019). Antibacterial activity of transition metal complexes containing a tridentate NNO phenoxymethylpenicillin-based Schiff base. An anti-MRSA iron (II) complex. *Applied Organometallic Chemistry*, *33*(4), e4744.
22. Abou-Melha, K. S., Al-Hazmi, G. A., Althagafi, I., Alharbi, A., Shaaban, F., El-Metwaly, N. M., ... & El-Bindary, M. A. (2021). Synthesis, characterization, DFT calculation, DNA binding and antimicrobial activities of metal complexes of dimedone arylhydrazone. *Journal of Molecular Liquids*, *334*, 116498.
23. Diaddario, L. L., Robinson, W. R., & Margerum, D. W. (1983). Crystal and molecular structure of tri-'s copper (III)-tripeptide complex of tri-. Alpha.-aminoisobutyric acid. *Inorganic Chemistry*, *22*(7), 1021-1025.
24. Heinert, D., & Martell, A. E. (1963). Pyridoxine and Pyridoxal Analogs. VII. Acid-Base Equilibria of Schiff Bases. *Journal of the American Chemical Society*, *85*(2), 188-193.
25. Çakır, Ü., Temel, H., İhan, S., & Uğraş, H. İ. (2003). Spectroscopic and conductance studies of new transition metal complexes with a Schiff base derived from 4-Methoxybenzaldehyde and 1, 2-bis (p-Aminophenoxy) ethane. *Spectroscopy letters*, *36*(5-6), 429-440.
26. Tian, W., Liao, H., Wu, J. G., & Yang, G. D. (1997). Study on the coordination of the hydroxyl group: crystal structure and FT-IR spectra of potassium hydrogen galactarate. *Polyhedron*, *16*(12), 2055-2058.
27. Thavamani, S. S., Amaladhas, T. P., AlSalhi, M. S., Devanesan, S., & Nicoletti, M. (2022). Transition metal complexes of 4-hydroxy-3-methoxybenzaldehyde embedded in fly ash zeolite as catalysts for phenol hydroxylation. *Chemosphere*, *289*, 133167.
28. Sunjuk, M., Al-Najjar, L., Shtaiwi, M., El-Eswed, B., Al-Noaimi, M., Al-Essa, L., & Sweidan, K. (2022). Transition Metal Complexes of Schiff Base Ligands Prepared from Reaction of Aminobenzothiazole with Benzaldehydes. *Inorganics*, *10*(4), 43.
29. Gao, L. G., Wang, H., Song, X. L., & Cao, W. (2013). Research on the chelation between luteolin and Cr (III) ion through infrared spectroscopy, UV–vis spectrum and theoretical calculations. *Journal of Molecular Structure*, *1034*, 386-391.
30. Butler, J. M., George, M. W., Schoonover, J. R., Dattelbaum, D. M., & Meyer, T. J. (2007). Application of transient infrared and near-infrared spectroscopy to transition metal complex excited states and intermediates. *Coordination Chemistry Reviews*, *251*(3-4), 492-514.
31. Natarajan, K., Poddar, R. K., & Agarwala, U. (1977). Mixed ruthenium (III) and ruthenium (II) complexes with triphenylphosphine or triphenylarsine and other ligands. *Journal of Inorganic and Nuclear Chemistry*, *39*(3), 431-435.
32. Maurya, R. C., Patel, P., & Rajput, S. (2003). Synthesis and Characterization of N-(o-Vanillinidene)-p-anisidine and N, N′-bis (o-Vanillinidene) ethylenediamine and Their Metal Complexes. *Synthesis and reactivity in inorganic and metal-organic chemistry*, *33*(5), 817-836.
33. Pawar, V. A. T. S. A. L. A., Uma, V., & Joshi, S. U. N. I. L. (2011). Synthesis, characterization and biological studies of Schiff bases metal complexes Co (II), Zn (II), Ni (II), and Mn (II) derived from amoxicillin trihydrate with various aldehydes. *Int J Pharm Bio Sci*, *2*, 240-250.
34. Singh, V. P. (2008). Synthesis, electronic and ESR spectral studies on copper (II) nitrate complexes with some acylhydrazines and hydrazones. *Spectrochimica Acta Part A: Molecular and Biomolecular Spectroscopy*, *71*(1), 17-22.
35. Amonovich, T. M., Nematovna, S. D., Giyasovich, A. K., Bafayevich, U. B., Shukurullayevich, G. B., & Qizi, S. N. Q. (2020). Synthesis and ESR Spectroscopy Complexes of Copper (II) with Acyl-and Aroylhydrazones of Methyl Ester of 5, 5-Dimethyl-2, 4-Dioxohexanoic Acid. *American Journal of Heterocyclic Chemistry*, *6*(2), 24-29.
36. Lund, A., Shiotani, M., & Shimada, S. (2011). *Principles and applications of ESR spectroscopy*. Springer Science & Business Media.
37. Tribollet, J., Galle, G., Jonusauskas, G., Deldicque, D., Tondusson, M., Létard, J. F., & Freysz, E. (2011). Transient absorption spectroscopy of the iron (II)[Fe (phen) 3] 2+ complex: Study of the non-radiative relaxation of an isolated iron (II) complex. *Chemical Physics Letters*, *513*(1-3), 42-47.
38. Liu, Y., Harlang, T., Canton, S. E., Chábera, P., Suárez-Alcántara, K., Fleckhaus, A., ... & Wärnmark, K. (2013). Towards longer-lived metal-to-ligand charge transfer states of iron (II) complexes: an N-heterocyclic carbene approach. *Chemical Communications*, *49*(57), 6412-6414.
39. Raman, N., Muthuraj, V., Ravichandran, S., & Kulandaisamy, A. (2003). Synthesis, characterisation and electrochemical behaviour of Cu (II), Co (II), Ni (II) and Zn (II) complexes derived from acetylacetone and ranitidine and their antimicrobial activity. *Journal of Chemical Sciences*, *115*, 161-167.
40. Konstantinovic, S. S., Radovanović, B., Cakic, Z., & Vasić, V. M. (2003). Synthesis and characterisation of Co (II), Ni (II), Cu (II) and Zn (II) complexes with 3-salicylidenehydrazono-2-indolinone. *Journal of the Serbian Chemical Society*, *68*(8-9), 641-647.

41. Liu, Z. C., Wang, B. D., Li, B., Wang, Q., Yang, Z. Y., Li, T. R., & Li, Y. (2010). Crystal structures, DNA-binding and cytotoxic activities studies of Cu (II) complexes with 2-oxo-quinoline-3-carbaldehyde Schiff-bases. *European journal of medicinal chemistry*, *45*(11), 5353-5361.
42. Chai, L. Q., Tang, L. J., Chen, L. C., & Huang, J. J. (2017). Structural, spectral, electrochemical and DFT studies of two mononuclear manganese (II) and zinc (II) complexes. *Polyhedron*, *122*, 228-240.
43. Chandra, S., & Gupta, K. (2002). Chromium (III), manganese (II), iron (III), cobalt (II), nickel (II) and copper (II) complexes with a pentadentate, 15-membered new macrocyclic ligand. *Transition Metal Chemistry*, *27*, 196-199.
44. P. Ghanghas, A. Choudhary, D. Kumar, K. Poonia, Coordination metal complexes with Schiff bases: Useful pharmacophores with comprehensive biological applications, Inorganic Chemistry Communications. 130 (2021) 130, 108710. doi:10.1016/j.inoche.2021.108710.
45. M. Bal, G. Ceyhan, B. Avar, M. Köse, A. Kayraldiz, M. Kurtoğlu, Synthesis and X-ray powder diffraction, electrochemical, and genotoxic properties of a new azo-Schiff base and its metal complexes, Turkish Journal of Chemistry. 38 (2014) 222–241. doi:10.3906/kim-1306-28.
46. M. Bouhdada, M. E. L. Amane, N. El Hamzaoui, Synthesis, spectroscopic studies, X-ray powder diffraction data and antibacterial activity of mixed transition metal complexes with sulfonate azo dye, sulfamate and caffeine ligands, Inorganic Chemistry = Communications. (2019). doi:10.1016/j.inoche.2019.01.005.
47. G. G. Mohamed, N. E. A. El-Gamel, Synthesis, investigation and spectroscopic characterization of piroxicam ternary complexes of Fe(II), Fe(III), Co(II), Ni(II), Cu(II) and Zn(II) with glycine and dl-phenylalanine, Spectrochimica Acta Part A: Molecular and Biomolecular Spectroscopy. 60.13 (2004) 3141–3154. doi:10.1016/j.saa.2004.01.035.
48. Psomas, G., Tarushi, A., Efthimiadou, E. K., Sanakis, Y., Raptopoulou, C. P., & Katsaros, N. (2006). Synthesis, structure and biological activity of copper (II) complexes with oxolinic acid. *Journal of Inorganic Biochemistry*, *100*(11), 1764-1773.
49. de Araújo, E. L., Barbosa, H. F. G., Dockal, E. R., & Cavalheiro, É. T. G. (2017). Synthesis, characterization and biological activity of Cu (II), Ni (II) and Zn (II) complexes of biopolymeric Schiff bases of salicylaldehydes and chitosan. *International journal of biological macromolecules*, *95*, 168-176.